Maximal-ratio eigen-combining: A performance analysis

Combinaison propre à rapport maximal : une analyse de la performance

Constantin Siriteanu and Steven D. Blostein*

Maximal-ratio eigen-combining (MREC) for wireless communications channels, also known as eigen-beamforming for receivers equipped with antenna arrays, integrates conventional maximum average signal-to-noise-ratio beamforming (Max-ASNR BF) and maximal-ratio combining (MRC) to provide both high average SNR in high fading correlation as well as diversity in low fading correlation. Previous studies of MREC were based on simulation or limited analysis and suggested that MREC can outperform Max-ASNR BF and MRC in terms of average error probability (AEP). A comprehensive analysis of MREC is provided for BPSK signals and Rayleigh fading, including computable AEP and outage probability (OP) expressions for perfectly known, correlated channel gains. Particular cases of these expressions apply to Max-ASNR BF and MRC. For imperfectly known channels the analysis yields a new and general AEP expression for MREC, which is specialized to estimation based on pilot-symbol-aided modulation (PSAM) and interpolation. In particular, this AEP expression applies to Max-ASNR BF and, for PSAM and data-independent interpolation filters, to MRC. Numerical results for antenna arrays receiving signals with angle-of-arrival dispersion and imperfectly known channel gains confirm the potential advantage of MREC over Max-ASNR BF and MRC.

La combinaison propre à rapport maximal (CPRM) pour des canaux de communication sans fil, également connue sous le nom de formation de faisceau propre pour des récepteurs équipés de réseaux d'antennes, intègre les méthodes conventionnelles de formation de faisceau maximisant le rapport moyen signal-à-bruit (FF Max-RMSB) et de combinaison à rapport maximal (CRM) et fournit à la fois de RMSB élevé en condition d'atténuation fortement corrélée et de la diversité en condition de basse corrélation de l'atténuation. Les études précédentes de la CPRM ont été basées sur la simulation ou sur une analyse limitée et ont suggérée que la CPRM puisse surpasser la FF Max-RMSB et la CRM en termes de probabilité moyenne d'erreur (PME). Une analyse complète de CPRM est donnée ici pour des signaux MP2E (modulation de phase à deux états) et d'atténuation Rayleigh, y compris des expressions calculables pour la PME et pour la probabilité de panne dans le cas de canaux parfaitement connus à gains corrélés. Pour des canaux imparfaitement connus, l'analyse apporte une expression nouvelle et générale de la PME pour la CPRM, qui est spécialisée à estimation assistée par modulation avec symbole pilote (MSP) et interpolation. Particulièrement, cette expression de la PME s'applique à la FF Max-RMSB et, dans le cas de MSP et de filtres d'interpolation indépendantes des données, à la CRM. Les résultats numériques pour des réseaux d'antennes recevant de signaux avec une dispersion d'angles d'arrivée et des gains de canaux imparfaitement connus confirment l'avantage potentiel de la CPRM par rapport à la FF Max-RMSB et à la CRM.

Keywords: beamforming, BPSK modulation, diversity, imperfectly known correlated channel gains, MRC, Rayleigh fading

I. Introduction

It is widely acknowledged that, for a perfectly known channel, maximal-ratio combining (MRC) [1] yields the lowest average error probability (AEP) in a diversity system if the (complex) channel gains are uncorrelated [1]–[5]. On the other hand, for antenna arrays with closely spaced elements, maximum average signal-to-noise-ratio beamforming [6] (Max-ASNR BF) yields the lowest AEP for coherent (completely correlated) channel gains [5], [7]. Since in an actual scenario the channel gains are not perfectly known and may never be completely uncorrelated or correlated, the principles of these approaches were recently integrated to create the more practical eigen-beamforming approach [5], denoted herein as maximal-ratio eigen-combining (MREC).

MREC consists of two steps: first, an appropriate number of dominant eigenvectors of the channel-vector correlation matrix are selected to form the Karhunen-Loève transform (KLT) [8], which is applied to the received signal vector [9]; then, MRC is applied to the resulting vector. Max-ASNR BF is clearly a special case of MREC which employs only the eigenvector corresponding to the largest eigenvalue [7], [10]. For a perfectly known channel, MRC of the received signal vector and MREC employing all eigenvectors (denoted further as *full MREC*) are equivalent [11], so that MRC may be viewed as a particular case of MREC. Simulation results [7], [10], [12]–[13] and limited analytical results [14] have suggested that MREC outperforms Max-ASNR BF when the channel gains are only partially correlated [7], [10], [12], and even MRC [12]–[14] for imperfectly known, correlated channel gains.

A comprehensive performance evaluation/comparison of MREC, Max-ASNR BF and MRC would require AEP and outage probability (OP) expressions for correlated channel gains that may have unequal variances and may be imperfectly known. The characteristic and moment generating functions (mgfs) of the output SNR or symbol detection variable were previously used to obtain performance measures (AEP, OP) for MRC, assuming perfectly known channel gains [2], [15]–[19] or estimated channel gains [20]–[21], and for MREC specifically for maximum-likelihood channel estimation [14]. However, previous analyses of MRC and MREC omitted or specified incompletely the AEP and OP in the case when some of the eigenvalues of the correlation matrix for the channel vector are equal. Since this situation may occur for signals received at antenna arrays [22] for various values of the angle-of-arrival (AOA) spread [23]–[24], it will be dealt with herein.

In this paper we analyze MREC for BPSK-modulated signals and wireless channel gains that undergo Rayleigh fading. In Section II, for perfectly known correlated channel gains, we examine MREC and its relationship with MRC and Max-ASNR BF, and we develop gen-

*Constantin Siriteanu and Steven D. Blostein are with the Department of Electrical and Computer Engineering, Queen's University, Kingston, Ontario K7L 3N6. E-mail: {costi, sdb}@ee.queensu.ca

eral AEP and OP expressions using the moment generating function of the instantaneous post-combining SNR. In particular, these expressions apply to MRC and Max-ASNR BF. In Section III, for imperfectly known correlated channel gains, we derive a novel and general AEP expression for MREC, based on the mgf of the symbol decision variable after combining. Channel estimation methods employing pilot-symbol-aided modulation (PSAM) and interpolation are discussed, and MRC and full MREC are found to be equivalent for data-independent interpolation. Numerical results drawn from analysis are shown in Section IV to support the claim that MREC may outperform both Max-ASNR BF and MRC when applied to signals received with angle-of-arrival dispersion at antenna arrays, for imperfectly known channels.

II. MREC with perfect channel knowledge

A. Signal model

Consider that L copies of a BPSK signal affected by Rayleigh fading and zero-mean additive white Gaussian noise (AWGN) are available for processing at the receiver. After demodulation, matched filtering and symbol-rate sampling, the complex-valued received signal vector can be written as

$$\tilde{\mathbf{y}} = \sqrt{E_b}\, b\, \tilde{\mathbf{h}} + \tilde{\mathbf{n}}, \tag{1}$$

where E_b is the energy transmitted per symbol, $b \in \{\pm 1\}$ is the equiprobable binary random symbol, and $\tilde{\mathbf{h}}$ and $\tilde{\mathbf{n}}$ are the complex zero-mean Gaussian channel and noise vectors, respectively, with $\tilde{\mathbf{h}} \sim \mathcal{N}(\mathbf{0}, \mathbf{R}_{\tilde{\mathbf{h}}})$ and $\tilde{\mathbf{n}} \sim \mathcal{N}(\mathbf{0}, N_0\, \mathbf{I}_L)$. We denote the elements of $\tilde{\mathbf{h}}$, i.e., the channel gains, as *branches*, and we assume them to be perfectly known throughout Section II.

The channel-vector correlation matrix $\mathbf{R}_{\tilde{\mathbf{h}}} \triangleq E\{\tilde{\mathbf{h}}\, \tilde{\mathbf{h}}^{\mathcal{H}}\}$ is Hermitian, i.e., $\mathbf{R}_{\tilde{\mathbf{h}}} = \mathbf{R}_{\tilde{\mathbf{h}}}^{\mathcal{H}}$, and therefore has real non-negative eigenvalues $\lambda_1 \geq \lambda_2 \geq \cdots \geq \lambda_L \geq 0$, and a complete set of orthonormal eigenvectors, $\mathbf{e}_i$, $i = 1 : L \triangleq 1, \ldots, L$. Then, $\mathbf{R}_{\tilde{\mathbf{h}}} = \mathbf{E}_L \mathbf{\Lambda}_L \mathbf{E}_L^{\mathcal{H}}$, where $\mathbf{\Lambda}_L \triangleq \text{diag}\{\lambda_i\}_{i=1}^{L}$ is a diagonal matrix and $\mathbf{E}_L \triangleq [\mathbf{e}_1\, \mathbf{e}_2\, \ldots\, \mathbf{e}_L]$ is a unitary matrix, i.e., $\mathbf{E}_L\, \mathbf{E}_L^{\mathcal{H}} = \mathbf{E}_L^{\mathcal{H}}\, \mathbf{E}_L = \mathbf{I}_L$. Throughout this work we assume that $\mathbf{\Lambda}_L$ and $\mathbf{E}_L$ are perfectly known.

B. MRC, Max-ASNR BF and MREC principles

Maximum average signal-to-noise-ratio beamforming [6] maximizes the average (over fading and noise) output SNR by combining the received signal with a vector proportional to the eigenvector of $\mathbf{R}_{\tilde{\mathbf{h}}}$ corresponding to its largest eigenvalue, i.e., $\mathbf{e}_1$. Maximal-ratio combining [1]–[3], [15]–[16], [25] maximizes the instantaneous (averaging over noise only) output SNR by combining the received signal vector with

$$\tilde{\mathbf{w}}_{\text{MRC}} = \tilde{\mathbf{h}}. \tag{2}$$

Maximal-ratio eigen-combining has two steps:

1. First, for an appropriately selected order $N \leq L$ [9], the KLT matrix $\mathbf{E}_N \triangleq [\mathbf{e}_1\, \mathbf{e}_2\, \ldots\, \mathbf{e}_N]$, with $\mathbf{E}_N^{\mathcal{H}}\, \mathbf{E}_N = \mathbf{I}_N$ and (for $N < L$) $\mathbf{E}_N\, \mathbf{E}_N^{\mathcal{H}} \neq \mathbf{I}_L$, is applied in (1), to obtain a transformed signal vector
$$\mathbf{y} = \sqrt{E_b}\, b\, \mathbf{h} + \mathbf{n}, \tag{3}$$
with $\mathbf{y} \triangleq \mathbf{E}_N^{\mathcal{H}}\, \tilde{\mathbf{y}}, \mathbf{h} \triangleq \mathbf{E}_N^{\mathcal{H}}\, \tilde{\mathbf{h}}, \mathbf{n} \triangleq \mathbf{E}_N^{\mathcal{H}}\, \tilde{\mathbf{n}}$. The elements h_i, $i = 1 : N$, of $\mathbf{h}$ are denoted as *eigen-branches* [5].
2. Then, MRC applied to the transformed signal vector $\mathbf{y}$ from (3) leads to eigen-beamforming [5], denoted herein as maximal-ratio eigen-combining. The corresponding combiner which maximizes the instantaneous output SNR for the signal in (3) is
$$\mathbf{w}_{\text{MREC}} = \mathbf{h}. \tag{4}$$

It can be shown that the *eigen-branches are mutually uncorrelated for any branch distribution* [8], and so they are *mutually independent, Gaussian* random variables with variances $E\{|h_i|^2\} = \lambda_i$ for our assumption of Rayleigh fading branches [11].

MRC of the original signal vector (denoted simply as MRC) is equivalent to MRC of the transformed signal vector when $N = L$ (denoted as *full MREC*) [11]. Therefore, if the original branches are correlated, performance measures for MRC can be derived simply, based on the equivalent full MREC for the independent eigen-branches [11]. On the other hand, MREC of order $N = 1$ is clearly Max-ASNR BF [7], [10].

Although MREC may look similar to hybrid selection combining/MRC (HSC/MRC) [15], [26]–[27], the two are actually significantly different. HSC/MRC was devised to reduce MRC complexity, and both are mainly targeted to scenarios with low branch correlations. MREC was devised as a better-performing but more-complex replacement of Max-ASNR BF for scenarios with only partially correlated branches [5], [7], [10]. Also, MREC was proposed as a better-performing and less-complex alternative to MRC in scenarios with partial correlation of the branches, when they may be poorly estimated [5], [12]–[14]. In *HSC/MRC* the *branches* with the strongest *instantaneous SNR* are processed, while in *MREC* the *eigen-branches* with the strongest *average SNR* are processed. Thus, for HSC/MRC the SNRs of all branches have to be estimated in the short term (shorter than the channel coherence time), while for MREC estimates of long-term (averaging over fading) SNRs are required.

C. MREC performance analysis for perfectly known channel

Given the MREC order $N \leq L$, let γ be the instantaneous SNR in $\mathbf{w}_{\text{MREC}}^{\mathcal{H}}\, \mathbf{y}$, and $p_\gamma(\gamma)$ its probability density function (pdf). Then, the average error probability for MREC is [15], [25]

$$P_e = E\{P_e(\gamma)\} = \int_0^\infty P_e(\gamma)\, p_\gamma(\gamma)\, d\gamma, \tag{5}$$

where $P_e(\gamma)$ is the error probability conditioned on the SNR. For BPSK, (5) leads to [15], [18]

$$P_e = \frac{1}{\pi} \int_0^{\pi/2} M_\gamma\left(\frac{1}{\sin^2\phi}\right) d\phi, \tag{6}$$

where $M_\gamma(s) \triangleq E\{e^{-s\gamma}\}$ is the moment generating function of γ.

The outage probability can be written as [15], [17], [19]

$$P_{\text{out}} = \int_0^{\gamma_{\text{th}}} p_\gamma(\gamma)\, d\gamma, \tag{7}$$

where γ_{th} is the SNR threshold. The OP can also be found using $M_\gamma(s)$ since $p_\gamma(\gamma)$ is its inverse Laplace transform.

The instantaneous SNR for the i-th eigen-branch is $\gamma_i \triangleq \frac{E_b}{N_0} |h_i|^2$, with average $E\{\gamma_i\} = \frac{E_b}{N_0}\lambda_i$ and exponential pdf [1], [15]

$$p_{\gamma_i}(\gamma_i) = \frac{1}{E\{\gamma_i\}}\, e^{-\frac{\gamma_i}{E\{\gamma_i\}}} \quad \text{for} \quad \gamma_i \geq 0, \tag{8}$$

so that the mgf of γ_i is

$$M_{\gamma_i}(s) \triangleq E\{e^{-s\,\gamma_i}\} = \frac{1}{1 + s \cdot E\{\gamma_i\}}. \tag{9}$$

For the combiner in (4) the total instantaneous SNR γ is maximized, i.e., $\gamma = \sum_{i=1}^{N} \gamma_i$ [1], [3].

In general, some eigenvalues of $\mathbf{R}_{\tilde{\mathbf{h}}}$ may coincide [22]. Therefore, let $\lambda'_1 > \lambda'_2 > \cdots > \lambda'_K$ denote the $K \leq N$ distinct eigenvalues, with algebraic multiplicities $r_1, r_2, \ldots, r_K$, respectively, where

$\sum_{k=1}^{K} r_k = N$. Then, because γ_i, $i = 1 : N$, are independent, the mgf of γ is

$$M_\gamma(s) = \prod_{k=1}^{K} \left(\frac{1}{1 + s\,\Gamma_k} \right)^{r_k}, \tag{10}$$

where $\Gamma_k \triangleq \frac{E_b}{N_0}\lambda'_k$, $k = 1 : K$, are the K distinct average SNRs for the eigen-branches. Then, for BPSK and Rayleigh fading branches which may be correlated and may have distinct average SNRs, the AEP expression for MREC can be determined by substituting (10) into (6) as

$$P_e = \frac{1}{\pi} \int_0^{\pi/2} \prod_{k=1}^{K} \left(\frac{\sin^2\phi}{\sin^2\phi + \Gamma_k} \right)^{r_k} d\phi. \tag{11}$$

This formula can be used to find the AEP for Max-ASNR BF as

$$P_{e,\mathrm{BF}} = \int_0^{\pi/2} \frac{\frac{1}{\pi}\sin^2\phi}{\sin^2\phi + \frac{E_b}{N_0}\lambda_1}\, d\phi = \frac{1}{2}\left(1 - \sqrt{\frac{\frac{E_b}{N_0}\lambda_1}{1 + \frac{E_b}{N_0}\lambda_1}} \right),$$

and to find the AEP for MRC for perfectly known branches which can be correlated, with unequal variances. Based on these formulas it can be shown that uncorrelated branches with equal variance minimize the AEP for MRC, while coherent branches maximize it. The opposite can be shown for Max-ASNR BF.

When the symbol SNR E_b/N_0 is large, the AEP for MREC becomes

$$P_{e,\text{high SNR}} = \frac{(2N)!}{2^{2N+1}(N!)^2} \cdot \left[\frac{E_b}{N_0} \right]^{-N} \cdot \prod_{i=1}^{N} \lambda_i^{-1}, \tag{12}$$

showing a diversity order equal to the number of combined eigen-branches, which is as expected, since they are independent.

Applying (11) for MRC of L independent and identically distributed (i.i.d.) branches, one can show that, given the total received intended energy, $\mathrm{tr}(\mathbf{R}_{\tilde{\mathbf{h}}})$, as L increases, the MRC AEP approaches

$$\lim_{L \longrightarrow \infty} P_e = Q\left(\sqrt{2\frac{E_b}{N_0}\mathrm{tr}(\mathbf{R}_{\tilde{\mathbf{h}}})} \right), \tag{13}$$

with $Q(x) \triangleq \int_x^\infty \frac{1}{\sqrt{2\,\pi}} e^{-\frac{y^2}{2}} dy = \frac{1}{\pi}\int_0^{\pi/2} e^{-\frac{x^2}{2}\frac{1}{\sin^2\phi}} d\phi$ [15, Eqs. (4.1)–(4.2)]. Note that the right-hand side of (13) is simply the error probability for a BPSK signal with symbol SNR equal to $\frac{E_b}{N_0}\mathrm{tr}(\mathbf{R}_{\tilde{\mathbf{h}}})$, transmitted through a nonfading channel with AWGN [25, Eq. (5.2-4)]. A similar conclusion is reached using another approach in [28, Eq. (17)]. Thus, an infinite number of i.i.d. diversity branches would make a Rayleigh fading single-input multiple-output channel equivalent to a nonfading single-input single-output channel with AWGN.

Performing numerical integration on (11) yields the AEP for any particular situation, for any values of the eigen-branch variances, i.e., the eigenvalues λ_i, $i = 1 : N$. The closed-form AEP expressions shown next do not require numerical integration, but each of them yields accurate results only when the assumed relationships among eigen-branch variances are valid.

1. *Equal-variance eigen-branches*

The AEP and OP expressions shown next form the building blocks for the other cases. For equal-variance eigen-branches, $K = 1, r_1 = N$ and $\Gamma_k = \Gamma$ reduce (10) to

$$M_\gamma(s) = \frac{1}{(1 + s\,\Gamma)^N}. \tag{14}$$

The inverse Laplace transform of (14) is the pdf of γ, and is given by [25, Eq. (14.4-13)]

$$p_\gamma(\gamma) = \frac{\gamma^{N-1} e^{-\frac{\gamma}{\Gamma}}}{(N-1)!\;\Gamma^N}, \tag{15}$$

so that, with the notation $\nu \triangleq \sqrt{\frac{\Gamma}{\Gamma+1}}$, the AEP is given by [25, Eq. (14.4-15)]

$$P_e = \left[\frac{1}{2}(1-\nu) \right]^N \sum_{n=0}^{N-1} \binom{N-1+n}{n} \left[\frac{1}{2}(1+\nu) \right]^n. \tag{16}$$

From (7) and (15), the OP is

$$P_{\text{out}} = \frac{\mathcal{G}\left(N; \frac{\gamma_{\text{th}}}{\Gamma} \right)}{(N-1)!}, \tag{17}$$

where $\mathcal{G}(n;x) \triangleq \int_0^x y^{n-1} e^{-y} dy$ is the incomplete gamma function [29, Eq. (8.350-1)].

Interestingly, it can be shown that if all eigen-branches have equal variance they actually are the original branches.

2. *Some eigen-branches have equal variance*

One can write the partial fraction expansion of the mgf in (10) as [29, §2.102, pp. 56–57]

$$M_\gamma(s) = \frac{1}{A} \sum_{k=1}^{K} \sum_{l=1}^{r_k} c_{k,l} \frac{1}{\left(s + \frac{1}{\Gamma_k} \right)^l}, \tag{18}$$

where $A \triangleq \prod_{k=1}^{K} \Gamma_k^{r_k}$,

$$c_{k,l} \triangleq \frac{A}{(r_k - l)!} \left\{ D_s^{(r_k - l)} \left[M_\gamma(s) \cdot \left(s + \frac{1}{\Gamma_k} \right)^{r_k} \right] \right\} \Big|_{s = -\frac{1}{\Gamma_k}},$$

and $D_s^{(n)}[G(s)] \triangleq \frac{d^n[G(s)]}{ds^n}$. Based on [30], $c_{k,l}$, $k = 1 : K$, $l = 1 : r_k$, can be expressed in closed form as

$$c_{k,l} = (-1)^{r_k - l} \cdot \sum_{\Omega} \prod_{\substack{j=1 \\ j \neq k}}^{K} d_j \cdot \left(\frac{1}{\Gamma_j} - \frac{1}{\Gamma_k} \right)^{-(r_j + i_j)}, \tag{19}$$

where Ω stands for the set of integers satisfying $0 \le i_1, \ldots, i_{k-1}, i_{k+1}, \ldots, i_K \le r_k - l$ and $i_1 + \cdots + i_{k-1} + i_{k+1} + \cdots + i_K = r_k - l$, and $d_j = \binom{r_j - 1 + i_j}{i_j}$.

If (18) is substituted into (6), a canonical form of the AEP for MREC is

$$P_e = \frac{1}{A} \sum_{k=1}^{K} \sum_{l=1}^{r_k} c_{k,l} \cdot \Gamma_k^l \cdot I_l(\Gamma_k), \tag{20}$$

where

$$I_l(\Gamma_k) = \frac{1}{\pi} \int_0^{\pi/2} \left[\frac{\sin^2\phi}{\sin^2\phi + \Gamma_k} \right]^l d\phi \tag{21}$$

is given by (16), by replacing ν with $\nu_k \triangleq \sqrt{\frac{\Gamma_k}{\Gamma_k + 1}}$, and N with l.

The inverse Laplace transform of the mgf in (18) results in the pdf of γ,

$$p_\gamma(\gamma) = \frac{1}{A} \sum_{k=1}^{K} \sum_{l=1}^{r_k} c_{k,l} \cdot \frac{\gamma^{l-1} e^{-\frac{\gamma}{\Gamma_k}}}{(l-1)!}, \tag{22}$$

which, substituted into (7), yields a canonical form of MREC OP as

$$P_{\text{out}} = \frac{1}{A}\sum_{k=1}^{K}\sum_{l=1}^{r_k} c_{k,l}\cdot\Gamma_k^l\cdot\frac{\mathcal{G}\left(l;\frac{\gamma_{\text{th}}}{\Gamma_k}\right)}{(l-1)!}. \tag{23}$$

In [19] a similar approach based on the characteristic function of γ yielded canonical forms of MRC AEP and OP for MPSK modulation and Nakagami-m fading, but these were incompletely specified. The above results can easily be extended to these modulation formats and fading distributions to yield completely specified AEP and OP expressions.

3. All eigen-branches have distinct variances

In this case $K = N$ and $r_k = 1, \forall k = 1 : N$, so that (18) and (19) yield [16, Eq. (10-59)]

$$M_\gamma(s) = \sum_{k=1}^{N} R_k\cdot\frac{1}{1+s\Gamma_k}, \tag{24}$$

where

$$R_k = \prod_{j\neq k}^{N}\frac{\Gamma_k}{\Gamma_k-\Gamma_j}. \tag{25}$$

Then, from (24), using (14) and (16) for $N = 1$, we obtain

$$P_e = \frac{1}{2}\sum_{k=1}^{N} R_k\cdot(1-\nu_k), \tag{26}$$

which is the MRC AEP formula [25, Eq. (14.5-28)] written for the N independent eigen-branches.

The pdf from (22) becomes [16, Eq. (10-60)]

$$p_\gamma(\gamma) = \sum_{k=1}^{N} R_k\cdot\frac{1}{\Gamma_k}e^{-\frac{\gamma}{\Gamma_k}}, \tag{27}$$

which corresponds to [25, Eq. (14.5-26)]. Then, the OP is

$$P_{\text{out}} = \sum_{k=1}^{N} R_k\cdot\left(1-e^{-\frac{\gamma_{\text{th}}}{\Gamma_k}}\right). \tag{28}$$

The AEP and OP formulas for MREC shown above for a perfectly known channel are completely specified, cover all scenarios and apply to Max-ASNR BF for $N = 1$ and to MRC for $N = L$.

III. MREC with imperfect channel knowledge

For BPSK and Rayleigh fading, we now analyze MREC when the eigen-branches are imperfectly known. The AEP expressions we derive are important since (a) they apply to Max-ASNR BF for $N = 1$ regardless of the estimation technique, and to MRC for $N = L$ for certain estimation methods; and (b) their numerical implementation shows that in practice MREC with $1 < N < L$ may yield improved symbol detection performance compared to Max-ASNR BF and MRC for channel gains which are partially correlated.

For an imperfectly known channel, the instantaneous output SNR alone is insufficient for finding the MRC AEP for BPSK modulation, as noted in [31, p. 55]. Therefore, for MREC we consider instead the decision variable for symbol detection [14], [20]–[21],

$$q \triangleq \Re\left\{\sum_{i=1}^{N} g_i^*\, y_i\right\} = \sum_{i=1}^{N}\Re\{g_i^*\, y_i\} = \sum_{i=1}^{N} q_i, \tag{29}$$

where $\Re\{\cdot\}$ stands for the real part of a complex number, $g_i \triangleq \hat{h_i}$ is the eigen-branch estimate, g_i^* stands for the complex conjugate of g_i, $y_i = \sqrt{E_b}\, b\, h_i + n_i$ is the i-th element of the transformed signal vector $\mathbf{y}$ from (3), and $q_i \triangleq \Re\{g_i^*\, y_i\}$.

We make the following assumptions: (a) the estimate g_i of the eigen-branch h_i is calculated from temporal samples of y_i, so that g_i and g_j are independent for $i \neq j$; (b) g_i is zero-mean; (c) g_i and h_i are jointly Gaussian; and (d) the correlation coefficient of g_i and h_i,

$$\mu_i \triangleq \frac{E\{h_i\, g_i^*\}}{\sqrt{E\{|h_i|^2\}\, E\{|g_i|^2\}}} = \frac{\sigma^2_{h_i,g_i}}{\sqrt{\sigma^2_{h_i}\,\sigma^2_{g_i}}} = \frac{\sigma^2_{h_i,g_i}}{\sqrt{\lambda_i\,\sigma^2_{g_i}}}, \tag{30}$$

is real-valued [25, Appendix C, Section C.3]. In Section III.B we will describe estimation approaches which satisfy these assumptions so that the following analysis applies.

A. MREC performance analysis for imperfectly known channel

Herein, we derive AEP expressions based on the following approach:

1. For symbol $b = 1$, the mgf of q_i, $M_{q_i}(s) \triangleq E\{e^{-s\,q_i}\}$, is computed.
2. Since q_i are independent, $i = 1 : N$, the mgf of q is determined as $M_q(s) \triangleq E\{e^{-s\,q}\} = \prod_{i=1}^{N} M_{q_i}(s)$, based on (29).
3. A partial fraction expansion of $M_q(s)$ may then be necessary before its inverse Laplace transform is taken to produce the pdf of q, $p_q(q)$.
4. The AEP is calculated as $P_e = \int_{-\infty}^{0} p_q(q)\, dq$.

As in Section II.C, we consider separately three particular situations.

1. Some eigen-branches have equal variance

Following steps 1 and 2 of the procedure outlined above, and assuming that some of the eigen-branches may have identical parameters, we derive the mgf of q as

$$M_q(s) = \prod_{k=1}^{K}\frac{1}{[-a_k^2(s-s_{k,1})(s+s_{k,2})]^{r_k}}, \tag{31}$$

where $a_k^2 = \frac{1}{4}N_0\,\sigma^2_{g_k}\left[1+(1-\mu_k^2)\,\Gamma_k\right]$ and

$$s_{k,\{1,2\}} = \frac{2\nu_k}{\sqrt{E_b\,\sigma^2_{h_k}\,\sigma^2_{g_k}}}\cdot\frac{1}{1\mp\mu_k\,\nu_k} \tag{32}$$

are both real and positive. The mgf in (31) is rewritten as

$$M_q(s) = \frac{1}{B}\prod_{p=1}^{2K}\frac{1}{(s+\sigma_p)^{\rho_p}}, \tag{33}$$

where $B = \prod_{k=1}^{K}(-a_k^2)^{r_k}$, $\sigma_p = -s_{p,1}$, $\rho_p = r_p$ for $p = 1 : K$, and $\sigma_p = s_{p-K,2}$, $\rho_p = r_{p-K}$ for $p = K+1 : 2K$. Using the same approach as in Section II.C.2, we obtain

$$M_q(s) = \frac{1}{B}\sum_{p=1}^{2K}\sum_{l=1}^{\rho_p} c_{p,l}\frac{1}{(s+\sigma_p)^l}, \tag{34}$$

with

$$\begin{aligned} c_{p,l} &\triangleq \frac{B}{(\rho_p-l)!}\left\{D_s^{(\rho_p-l)}\left[M_q(s)\cdot(s+\sigma_p)^{\rho_p}\right]\right\}\Big|_{s=-\sigma_p} \\ &= (-1)^{\rho_p-l}\cdot\sum_{\Psi}\prod_{\substack{j=1\\ j\neq p}}^{2K}\delta_j\cdot\frac{1}{(\sigma_j-\sigma_p)^{(\rho_j+i_j)}}, \end{aligned} \tag{35}$$

where Ψ stands for the set of integers satisfying $0 \leq i_1, \ldots, i_{p-1}, i_{p+1}, \ldots, i_{2K} \leq \rho_p - l$ and $i_1 + \cdots + i_{p-1} + i_{p+1} + \cdots + i_{2K} = \rho_p - l$, and $\delta_j = \binom{\rho_j - 1 + i_j}{i_j}$.

The pdf of q can be obtained as the inverse Laplace transform of (34),

$$p_q(q) = \frac{1}{B} \sum_{k=1}^{K} \sum_{l=1}^{r_k} \left[-\frac{c_{k,l}}{(l-1)!} q^{l-1} e^{s_{k,1} q} u(-q) + \frac{c_{k+K,l}}{(l-1)!} q^{l-1} e^{-s_{k,2} q} u(q) \right], \quad (36)$$

where $u(q) = 0$ for $q < 0$, and $u(q) = 1$ for $q \geq 0$. Then,

$$P_e = \frac{1}{B} \sum_{k=1}^{K} \sum_{l=1}^{r_k} c_{k,l} \cdot \left[-\frac{\sqrt{E_b \sigma_{h_k}^2 \sigma_{g_k}^2}}{\nu_k} \cdot \frac{1 - \mu_k \nu_k}{2} \right]^l. \quad (37)$$

This novel formula is applicable for arbitrary correlations between the original branches and for any estimation method which satisfies the assumptions made earlier for the distribution of the eigen-branches and their corresponding estimates. MREC AEP plots obtained by specializing the above formula to estimation methods described in Section III.B will be discussed in Section IV.

2. *Equal-variance eigen-branches*

In this case we drop the index k because $k = K = 1$ ($r_1 = N$), and manipulate (37) using (35) to obtain

$$P_e = \left[\frac{1 - \mu\nu}{2} \right]^N \sum_{n=0}^{N-1} \binom{N-1+n}{n} \left[\frac{1 + \mu\nu}{2} \right]^n. \quad (38)$$

This equation can be shown to coincide with [20, Eq. (59)] written for the independent eigen-branches. For perfectly known eigen-branches we have $\mu = 1$, and (38) reduces to the well-known result [25, Eq. (14.4-15)] written for the independent eigen-branches.

3. *All eigen-branches have distinct variances*

In this case, $K = N$ and $r_k = 1, \forall k = 1 : N$, so that (37) and (35) yield

$$P_e = \frac{1}{2} \sum_{k=1}^{N} S_k \cdot (1 - \mu_k \nu_k), \quad (39)$$

where

$$S_k = \prod_{\substack{j=1 \\ j \neq k}}^{N} \frac{1}{a_j^2 (s_{j,1} - s_{k,1})(s_{j,2} + s_{k,1})}. \quad (40)$$

From (39) and (40) one can obtain the MREC AEP expression [14, Eq. (16)] which was derived specifically for unequal eigen-branch variances (eigenvalues) and for maximum-likelihood (ML) estimation. Unlike (39), the novel AEP expression in (37) can be applied in any correlation scenario, as will be illustrated in Section IV.

Note that for $N = 1$ the AEP expressions derived above hold for Max-ASNR BF, while for $N = L$ they may hold for MRC, as claimed below.

PROPOSITION: *For estimated branches and eigen-branches, MRC is equivalent to full MREC if and only if*

$$\widehat{\mathbf{E}_L^{\mathcal{H}} \tilde{\mathbf{h}}} = \mathbf{E}_L^{\mathcal{H}} \hat{\mathbf{h}}, \quad (41)$$

where $\hat{\cdot}$ denotes an estimator. The proof follows by imposing equality between the combiners' outputs for MRC and MREC.

Table 1
Interpolation filters

SINC	$[\mathbf{v}_i(m)]_t = \text{sinc}(\frac{m}{M} - t) \frac{\cos[\pi\beta(\frac{m}{M} - t)]}{1 - [2\beta(\frac{m}{M} - t)]^2} = [\mathbf{v}(m)]_t$
MMSE	$\mathbf{v}_i(m) = \mathbf{\Phi}_i^{-1} \boldsymbol{\phi}_i(m)$

Table 2
Elements of $\mathbf{\Phi}_i$ and $\boldsymbol{\phi}_i(m)$

$[\mathbf{\Phi}_i]_{t_1,t_2}$	$\lambda_i J_0(2\pi f_n \lvert t_1 - t_2 \rvert M) + \frac{N_0}{E_b \lvert b_p \rvert^2} \delta_{t_1,t_2}$
$[\boldsymbol{\phi}_i(m)]_t$	$\lambda_i J_0(2\pi f_n \lvert tM - m \rvert)$

Clearly, if the original branches are uncorrelated, then $\mathbf{E}_L = \mathbf{I}_L$ in (41), and the above AEP expressions describe MRC for independent branches with unequal or equal variances for any estimation method. The case of correlated branches is discussed in the following section.

B. Estimation using PSAM and interpolation

In pilot-symbol-aided modulation the transmitter periodically inserts pilot symbols into the data symbol stream. The receiver then estimates the channel gain by interpolating the pilot samples acquired across frames [32].

The notation (t, m) is used to denote temporal indexing, where $t = -T_1 : T_2$ is the frame index, t = 0 corresponds to the frame in which estimation takes place, $T = T_1 + T_2 + 1$ frames are used for interpolation, and $m = 0 : M - 1$ is the symbol index within the frame, where $m = 0$ corresponds to the pilot symbol and M is the frame length. For MREC, the estimate of the i-th eigen-branch at the m-th data symbol position in the current frame can be written based on [32] as

$$g_i(0, m) = \mathbf{v}_i(m)^{\mathcal{H}} \mathbf{r}_i, \quad (42)$$

where $\mathbf{v}_i(m)$ contains the interpolation coefficients and is denoted as the PSAM interpolation filter, and $\mathbf{r}_i$ is a vector formed with the pilot signal samples:

$$\mathbf{r}_i \triangleq \frac{1}{\sqrt{E_b} b_p} [y_i(-T_1, 0) \ \ldots \ y_i(T_2, 0)]^{\top}, \quad (43)$$

where b_p is the pilot symbol and $y_i(t, 0) = \mathbf{e}_i^{\mathcal{H}} \tilde{\mathbf{y}}(t, 0)$.

The interpolation filters can be classified as

1. *data-independent*, e.g., the filter with brick-wall-type frequency response, which is optimum in the absence of noise; we will refer to this filter, with impulse response tapered by a raised-cosine window [33], as the SINC filter, and the corresponding estimation approach as SINC PSAM;
2. *data-dependent*, e.g., the Wiener filter, which is minimum mean-squared error (MMSE) optimum in the presence of noise, but requires the second-order statistics of the received signals [32]; this filter is referred to as the MMSE filter, and the corresponding estimation approach as MMSE PSAM.

Table 1 specifies the SINC [33] and MMSE [32] interpolation filters, where $\text{sinc}(x) = \frac{\sin \pi x}{\pi x}$ and β is the roll-off factor ($\beta = 0.2$ for the numerical results shown later); the elements of matrix $\mathbf{\Phi}_i \triangleq E\{\mathbf{r}_i \mathbf{r}_i^{\mathcal{H}}\}$ and of vector $\boldsymbol{\phi}_i(m) \triangleq E\{\mathbf{r}_i h_i^*(0, m)\}$ are expressed for Jakes' model of temporal correlation [3] in Table 2, with $J_0(\cdot)$ representing the zeroth-order Bessel function of the first kind, and f_n the normalized maximum Doppler rate.

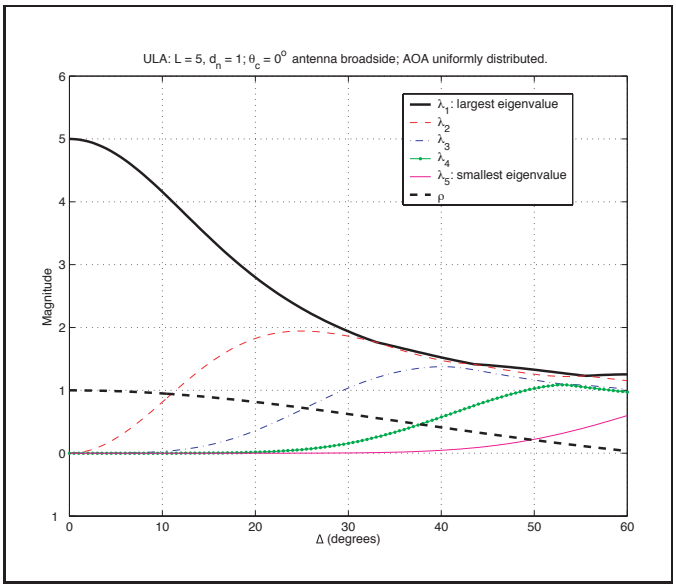

Figure 1: *The eigenvalues λ_i, $i = 1 : L$, of the channel-vector correlation matrix $\mathbf{R}_{\tilde{\mathbf{h}}}$, and the fading correlation coefficient ρ at any two adjacent antenna elements vs. the maximum AOA dispersion, Δ, for uniformly distributed AOA.*

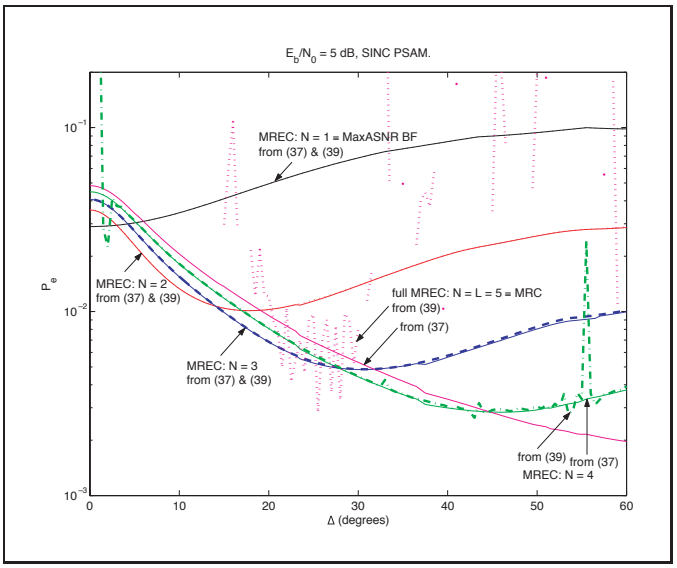

Figure 2: *MREC AEP vs. Δ, for SINC PSAM channel estimation; the AEP computed with (37) is plotted with solid lines, and the AEP computed with (39) is plotted with dashed/dotted lines.*

Table 3
Correlations required for μ_i in (30)

$\sigma^2_{h_i}$	λ_i
$\sigma^2_{h_i,g_i}$	$\boldsymbol{\phi}_i(m)^{\mathcal{H}}\mathbf{v}_i(m)$
$\sigma^2_{g_i}$	$\mathbf{v}_i(m)^{\mathcal{H}}\boldsymbol{\Phi}_i\,\mathbf{v}_i(m)$

Based on (42) and (43), the correlations required to compute μ_i from (30) and the MREC AEPs from Section III.A were determined and are shown in Table 3. Notice that the AEP will depend on the symbol position in the frame [32].

For correlated branches and data-independent interpolation filters (such as ML [13, Eq. (9)] or SINC), straightforward calculations can show that (41) is satisfied such that full MREC is equivalent to MRC, so that, for $N = L$, the AEP expressions derived in Section III.A apply to MRC. For (data-dependent) MMSE interpolation we found through slightly more complicated calculations that (41) is not satisfied, so that full MREC is not equivalent to MRC in this case.

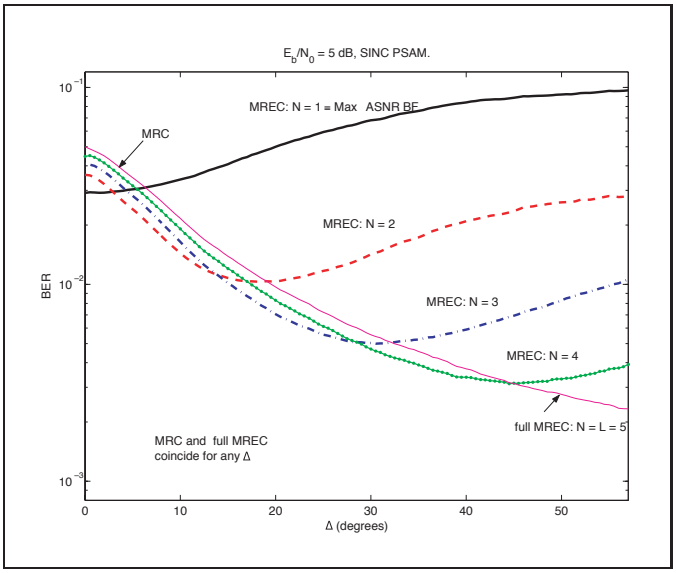

Figure 3: *MRC and MREC BER vs. Δ, obtained by simulation, for SINC PSAM channel estimation.*

IV. Numerical results

In this section, we consider that the vector $\tilde{\mathbf{y}}$ in (1) is formed with the signals received at L elements of a uniform linear array (ULA). The normalized inter-element distance is defined as $d_n = \frac{d}{\lambda/2}$, where d is the physical inter-element distance and λ is the carrier wavelength. We assume that the transmitted signal may undergo scattering during propagation and reaches the antenna array with an angle of arrival which has uniform distribution [23, Eq. (8)] in the interval $[\theta_c - \Delta, \theta_c + \Delta]$, where θ_c is the central AOA measured with respect to antenna broadside, and Δ is the maximum AOA dispersion. Unless stated otherwise, the following results are for $d_n = 1$ (a common choice for beamforming antennas [6]), $L = 5$, and $\theta_c = 0^\circ$.

The eigenvalues of the channel-vector correlation matrix and the fading correlation coefficient for any two adjacent antenna elements can be calculated using [23, Eqs. (A-19)–(A-20)], and are plotted versus Δ in Fig. 1. Notice that for small Δ the received signals are highly correlated and the intended-signal energy, i.e., $\text{tr}(\mathbf{R}_{\tilde{\mathbf{h}}}) = \sum_{i=1}^{L} \lambda_i$, is concentrated in the first few eigenvalues. As Δ increases, the correlation decreases and the energy is spread more uniformly over the eigen-branches. Notice also that some eigenvalues may be equal for certain Δ values, which suggests that the new AEP and OP expressions derived in previous sections would be required.

We present numerical results for Rayleigh fading with maximum normalized Doppler rate $f_n = 0.05$, and eigen-branches estimated using PSAM and interpolation with $M = 7$ and $T = 11$ ($T_1 = T_2 = 5$) [32]. Note that all shown error probabilities result from averaging over a frame of symbols.

Fig. 2 shows the MREC AEP versus Δ for SINC PSAM and symbol SNR $E_b/N_0 = 5$ dB. The solid lines are obtained by computing AEP using (37), i.e., by allowing some of the poles of the mgf in (34) to be equal, while the dashed/dotted lines are obtained by computing the AEP using (39), i.e., assuming that all the poles of the mgf in (34) are distinct. Clearly, when some of the eigenvalues are equal, (39) does not provide useful results. For instance, the plot obtained from (39)

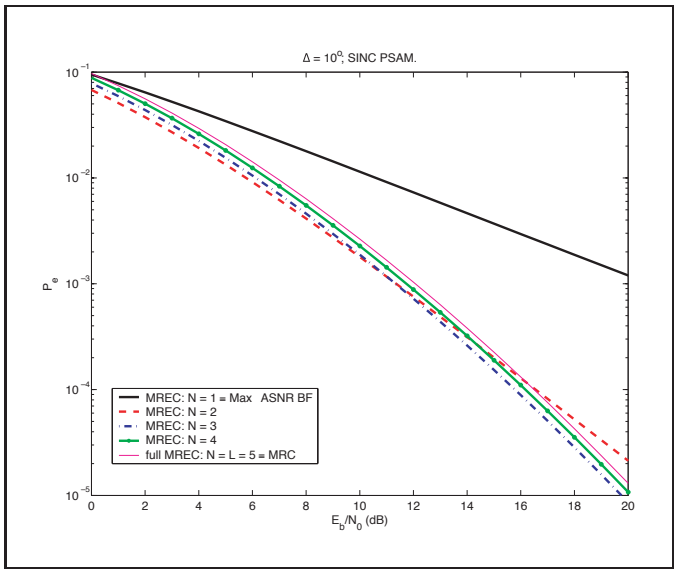

Figure 4: *MREC AEP obtained with (37) vs. the symbol SNR E_b/N_0, for SINC PSAM channel estimation and $\Delta = 10°$.*

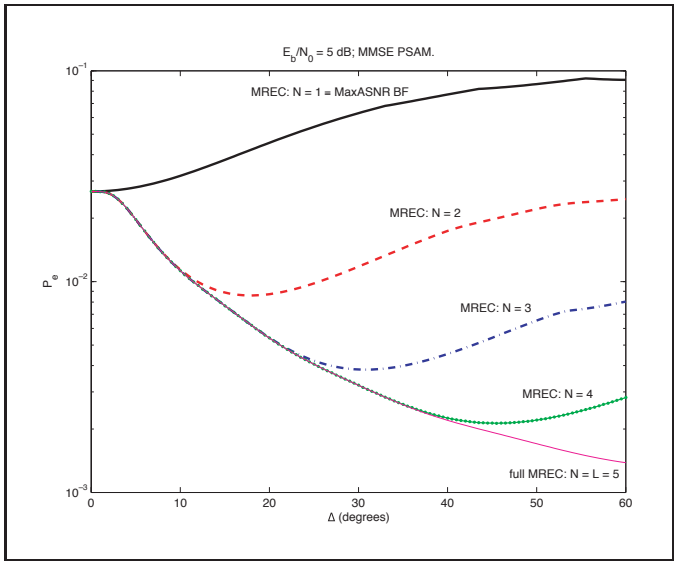

Figure 5: *MREC AEP obtained with (37) vs. Δ, for MMSE PSAM channel estimation.*

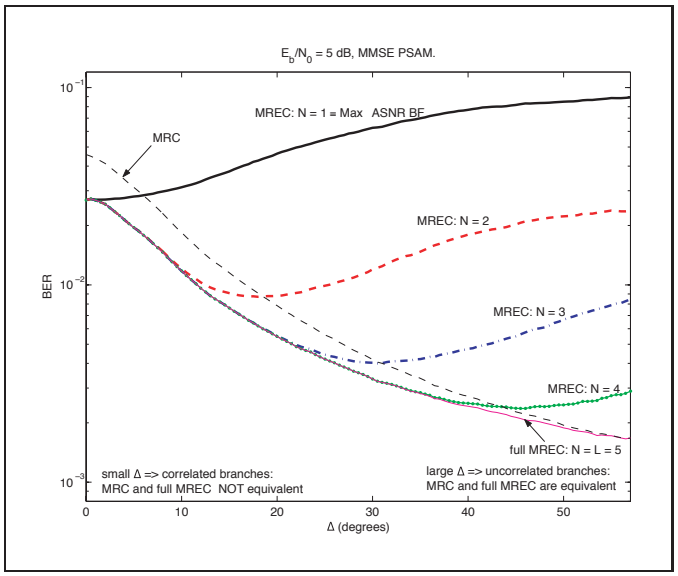

Figure 6: *MRC and MREC BER vs. Δ, obtained by simulation, for MMSE PSAM channel estimation.*

for full MREC is discontinuous because the assumption of unequal eigenvalues leading to (39) is violated at many values of Δ, as seen in Fig. 1. Notice that as N decreases, the plots obtained from (39) are less affected by this problem, which is as expected, considering Fig. 1. Nevertheless, the AEP curves obtained using (37) and shown in Fig. 2 closely match the bit error rate (BER) simulation results shown in Fig. 3, for any Δ. Thus, (37) can be employed to evaluate MREC in any scenario, unlike previously derived AEP expressions [14], [20].

Most importantly, Figs. 1, 2 and 3 show that, for SINC PSAM, Max-ASNR BF (which is MREC with $N = 1$) yields the lowest AEP when the branches are highly correlated. However, MREC with $N > 2$ yields much lower AEP than Max-ASNR BF when the branches are only partially correlated, as is also observed by simulation in [7] and [12]. Note also that MREC with $N < L$ may even outperform MRC (equivalent to full MREC for SINC PSAM), since the former combines only the N eigen-branches with highest average SNR, while the latter combines virtually all eigen-branches.

These observations are further illustrated in Fig. 4, where the AEP computed using (37) is depicted versus the symbol SNR for $\Delta = 10°$. Note that for $P_e = 10^{-2}$, MREC with $N = 2$ has an advantage of almost 5 dB compared to Max-ASNR BF and over 1 dB compared to MRC. Furthermore, this figure shows that, besides the fading correlation, the symbol SNR, which impacts the quality of the estimates, is also an important factor determining the relative performance of MREC, Max-ASNR BF and MRC, as noted in [14]. Ideally, the processing algorithm controlling a smart antenna system should adaptively choose the best combining approach for the encountered channel. In [9] we described a method which trades off detection performance and complexity in selecting the MREC order.

For the case of MMSE PSAM estimation, Fig. 5 shows MREC AEP plots obtained using (37). These results match the simulation results presented in Fig. 6 quite closely. These figures show that for correlated branches MRC is not equivalent to full MREC, a result which should be expected because (41) does not hold for MMSE PSAM. Once again, for $1 < N < L$, the performance advantage of MREC over Max-ASNR BF and MRC may be significant.

Notice from Figs. 2 and 3 that for SINC PSAM, given Δ, the symbol detection performance may degrade when the MREC order is increased. This happens because the eigen-branch estimate corresponding to a very small eigenvalue is mainly due to the corresponding noise and may not be close to zero for SINC PSAM, as seen from (42) and Tables 1 and 2. For MMSE PSAM such eigen-branches will have a correspondingly small contribution to the combiner's output, and therefore MREC performance always improves with increasing order, as suggested by the plots in Figs. 5 and 6.

Let us now consider a larger normalized inter-element distance, e.g., $d_n = 3$. For $\Delta = 10°$ and $\theta_c = 0°$, the correlation coefficient for two adjacent branches was found to be about 0.6, making MRC appropriate for this particular situation. However, for $\theta_c = 60°$ the correlation coefficient increases to about 0.9. This result is consistent with observations from [23] and [24]. For SINC PSAM, Fig. 7 shows that at $P_e = 10^{-2}$, MREC with $N = 3$ yields an advantage of about 0.75 dB over MRC. Since MRC and full MREC are equivalent for SINC PSAM, the method devised in [9] can be used to select the MREC order which will ensure near-optimal detection performance and low complexity.

Finally, we note that although the numerical results shown herein are for uniform AOA distribution, we also considered the case of Laplacian AOA distribution [24] and obtained similar results which are not shown.

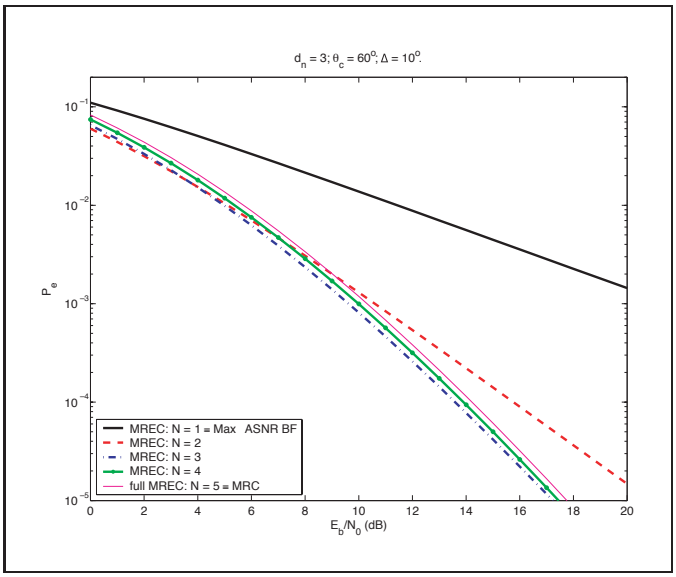

Figure 7: *MREC AEP obtained with (37) vs. the symbol SNR E_b/N_0, for SINC PSAM channel estimation, when $d_n = 3$, $\theta_c = 60°$ and $\Delta = 10°$.*

V. Conclusions

In this paper we analyzed maximal-ratio eigen-combining for Rayleigh fading channels and BPSK signals. For perfectly known, correlated channel gains which may have unequal variances, we obtained average error probability and outage probability expressions for MREC, with MRC and Max-ASNR BF as special cases. For imperfectly known, correlated channel gains we derived a novel and general AEP expression for MREC, which was further specialized for fading gain estimation based on pilot-symbol-aided modulation and interpolation. In particular, the result applies to Max-ASNR BF, and to MRC for correlated channels which are estimated using PSAM and data-independent interpolation. The results of our analysis are investigated numerically for antenna arrays receiving signals with uniformly distributed angle of arrival. Significant gains are observed with MREC over Max-ASNR BF and MRC for moderately correlated, imperfectly known channel gains.

Acknowledgements

This research has been sponsored by the Natural Sciences and Engineering Research Council of Canada, grant 41731-00, by Bell University Labs and by Samsung AIT.

References

[1] D.G. Brennan, "Linear diversity combining techniques," *Proc. IEEE*, vol. 91, no. 2, Feb. 2003, pp. 331–356.

[2] J.N. Pierce and S. Stein, "Multiple diversity with nonindependent fading," *Proc. IRE*, vol. 48, no. 1, Jan. 1960, pp. 89–104.

[3] W.C. Jakes, *Microwave Mobile Communications*, New York: John Wiley and Sons, 1974.

[4] L.-F. Tsaur and D.C. Lee, "Comments on MRC performance for M-ary modulation in arbitrarily correlated Nakagami fading channels," *IEEE Commun. Lett.*, vol. 6, no. 11, Nov. 2002, pp. 490.

[5] J.S. Hammerschmidt, C. Brunner, and C. Drewes, "Eigenbeamforming—A novel concept in array signal processing," in *Proc. European Wireless Conf. 2000*, Sept. 2000, Dresden, Germany. Available from World Wide Web: <http://www.lis.ei.tum.de/research/lm/e_publ.html>.

[6] R.A. Monzingo and T.W. Miller, *Introduction to Adaptive Arrays*, New York: John Wiley, 1980.

[7] M. Kim, W.-C. Lee, J. Choi, and S. Choi, "Adaptive beamforming technique based on eigen-space method for a smart antenna in IS2000 1X environment," in *Proc. Antennas and Propagat. Society Int. Symp.*, vol. 1, 2002, pp. 118–121.

[8] R.A. Haddad and T.W. Parsons, *Digital Signal Processing: Theory, Applications, and Hardware*, New York: Computer Science Press (an imprint of W.H. Freeman and Co.), 1991.

[9] Constantin Siriteanu and Steven D. Blostein, "Performance of smart antenna arrays with maximal-ratio eigencombining" [online], Technical Report 0401, Kingston, Ont.: Department of Electrical and Computer Engineering, Queen's University, 2004 [cited Mar. 31, 2004], available from World Wide Web: <http://ipcl.ee.queensu.ca/PAPERS/papers_online.html>.

[10] J. Choi and S. Choi, "Diversity gain for CDMA systems equipped with antenna arrays," *IEEE Trans. Veh. Technol.*, vol. 52, no. 3, May 2003, pp. 720–725.

[11] X. Dong and N.C. Beaulieu, "Optimal maximal ratio combining with correlated diversity branches," *IEEE Commun. Lett.*, vol. 6, no. 1, Jan. 2002, pp. 22–24.

[12] C. Brunner, W. Utschick, and J.A. Nossek, "Exploiting the short-term and long-term channel properties in space and time: Eigenbeamforming concepts for the BS in WCDMA," *European Trans. Telecommun.* (special issue on smart antennas), vol. 12, no. 5, 2001, pp. 365–378.

[13] F. Dietrich and W. Utschick, "On effective spatio-temporal rank of wireless communication channels," in *Proc. 13th IEEE Int. Symp. Personal, Indoor and Mobile Radio Commun.*, vol. 5, Sept. 2002, pp. 1982–1986.

[14] ———, "Maximum ratio combining of correlated Rayleigh fading channels with imperfect channel knowledge," *IEEE Commun. Lett.*, vol. 7, no. 9, Sept. 2003, pp. 419–421.

[15] M.K. Simon and M.-S. Alouini, *Digital Communication over Fading Channels: A Unified Approach to Performance Analysis*, New York: John Wiley and Sons, 2000.

[16] W.C.Y. Lee, *Mobile Communications Engineering*, New York: McGraw-Hill, 1982.

[17] P. Lombardo, G. Fedele, and M.M. Rao, "MRC performance for binary signals in Nakagami fading with general branch correlation," *IEEE Trans. Commun.*, vol. 47, no. 1, Jan. 1999, pp. 44–52.

[18] Y. Ma, C.C. Chai, and T.J. Lim, "Unified analysis of error probability for MRC in correlated fading channels," *Electron. Lett.*, vol. 35, no. 16, Aug. 1999, pp. 1314–1315.

[19] M.Z. Win and J.H. Winters, "On maximal ratio combining in correlated Nakagami channels with unequal fading parameters and SNRs among branches: An analytical framework," in *Proc. Wireless Communications and Networking Conf.*, vol. 3, Sept. 1999, pp. 1058–1064.

[20] P. Bello and B.D. Nelin, "Predetection diversity combining with selectively fading channels," *IRE Trans. Commun. Syst.*, vol. 10, no. 1, Mar. 1962, pp. 32–42.

[21] D. Singh, A. Kumari, R.K. Mallik, and S.S. Jamuar, "Analysis of rake reception with MRC and imperfect weight estimation for binary coherent orthogonal signaling," *IEEE Commun. Lett.*, vol. 6, no. 6, June 2002, pp. 245–247.

[22] J. Hammerschmidt and C. Brunner, "Merging diversity and beamforming perceptions in spatial signal processing," *Frequenz*, no. 5/6, May/June 2001. Available from World Wide Web: <http://www.chrisbrunner.org/publications/frequenz8.pdf>.

[23] J. Salz and J.H. Winters, "Effect of fading correlation on adaptive arrays in digital mobile radio," *IEEE Trans. Veh. Technol.*, vol. 43, no. 4, Nov. 1994, pp. 1049–1057.

[24] J.-A. Tsai, M. Buehrer, and B. Woerner, "The impact of AOA energy distribution on the spatial fading correlation of linear antenna array," in *Proc. 58th IEEE Veh. Technol. Conf.*, vol. 2, May 2002, pp. 933–937.

[25] J.H. Proakis, *Digital Communications*, 4th ed., Boston, Mass.: McGraw-Hill, 2001.

[26] Y. Ma and C.C. Chai, "Unified error probability analysis for generalized selection combining in Nakagami fading channels," *IEEE J. Select. Areas Commun.*, vol. 18, no. 11, Nov. 2000, pp. 2198–2210.

[27] A. Annamalai and C. Tellambura, "Analysis of hybrid selection/maximal-ratio diversity combiners with Gaussian errors," *IEEE Trans. Wireless Commun.*, vol. 1, no. 3, July 2002, pp. 498–512.

[28] D.V. Djonin, P. Tarasak, and V.K. Bhargava, "On the influence of the power profile on diversity combining schemes," in *Proc. IEEE Global Telecommun. Conf., GLOBECOM '03*, vol. 3, Dec. 2003, pp. 1659–1663.

[29] I.S. Gradshteyn and I.M. Ryzhik, eds., *Tables of integrals, Series and Products*, 4th ed., New York: Academic Press, 1965.

[30] S.V. Amari and R.B. Misra, "Closed-form expressions for distribution of sum of exponential random variables," *IEEE Trans. Rel.*, vol. 46, no. 4, Dec. 1997, pp. 519–522.

[31] B.R. Tomiuk, *Effects of Imperfect Maximal Ratio Combining on Digital Communications*, Ph.D. dissertation, Queen's University, Kingston, Ont., Sept. 2002.

[32] J.K. Cavers, "An analysis of pilot symbol assisted modulation for Rayleigh fading channels," *IEEE Trans. Veh. Technol.*, vol. 40, no. 4, Nov. 1991, pp. 686–693.

[33] N.W.K. Lo, David D. Falconer, and A.U.H. Sheikh, "Adaptive equalization and diversity combining for mobile radio using interpolated channel estimates," *IEEE Trans. Veh. Technol.*, vol. 40, no. 3, Aug. 1991, pp. 636–645.